Composite Structures 206 (2018) 164–176

Contents lists available at ScienceDirect

Composite Structures

journal homepage: www.elsevier.com/locate/compstruct

Integrative hinge based on shape memory polymer composites: Material, design, properties and application

Tianzhen Liu[a], Liwu Liu[b], Miao Yu[c], Qifeng Li[a], Chengjun Zeng[a], Xin Lan[a], Yanju Liu[b], Jinsong Leng[a,*]

[a] Centre for Composite Materials and Structures, Harbin Institute of Technology (HIT), No. 2 YiKuang Street, PO Box 3011, Harbin 150080, People's Republic of China
[b] Department of Astronautical Science and Mechanics, Harbin Institute of Technology (HIT), No. 92 West dazhi Street, PO Box 301, Harbin 150001, People's Republic of China
[c] Shanghai Institute of Satellite Engineering, No. 3666 Yuanjiang Street, Shanghai 201109, People's Republic of China

ARTICLE INFO

Keywords:
Shape memory polymer composites
Integrative hinge
Bending behavior
Variable stiffness

ABSTRACT

Self-deployable structures based on shape memory polymer composites (SMPCs) have the capability of self-deploy, light weight and high load-bearing. This paper presents the detail of an integrative hinge fabricated by carbon fiber reinforced shape memory epoxy composites in the sequence of material selection, structure design and manufacture, material and structure experiments, and application. DMA experiments have been conducted to figure out the temperature sensitivity of SMP. The temperature dependent elastic modulus and strength of SMPC were determined by tensile experiments. Results from three point bending tests and shape memory recovery tests verify the variable stiffness of the integrate SMPC hinge under different temperatures and superior shape memory properties. Strain distribution during bending process are obtained from both digital image correlation (DIC) measurements and ABAQUS simulation, showing good consistency with each other. To compare the modal characteristics with traditional SMPC hinge, modal testing and computation have been designed with free boundary condition. It can be found that the integrative SMPC hinges have the characteristics of improved reliability and performance, and higher post-deployment stiffness and strength, when compared to traditional SMPC hinges. Finally, prospective applications of the self-deployable structure have also been illustrated.

1. Introduction

Shape memory polymer (SMP) refers to a kind of intelligent material which is capable of perceiving external actuations, making active responses and shape memory effect [1–3]. SMP can deform from the temporary shape, which is formed by external force, to the initial shape when exposed to the specific stimulus, such as thermal, electrical, alternating magnetic fields, light and water stimulus [2,4–7]. The mechanisms of shape memory effect result from the glass transition or melting transition of molecular chains in SMP. Compared with shape memory alloys, SMP and SMPCs have distinctive advantages, including simple manufacturing process, light weight, large deformation ability and biological adaptability [8–10]. SMP and SMPCs have shown broad application prospect and development potential in manufacture of space deployable structures, medical devices, artificial muscles, breathable clothing and sensors [11–14].

Deployable structures are necessary components in various industries [15]. Especially in aerospace [16], navigation, weapon and equipment structure fields [17,18], the applications have attracted more and more extensive attention and recognition. In general, traditional deployable components rely on spring driven and mechanical driven systems [19,20], which are quite complicated and lead to serious impact to the whole structure inevitably with relatively heavy shocks and vibrations when deploying. In order to overcome these problems, intelligent deployable structures based on SMPCs have been adopted to realize the capabilities of structure bearing, self-locking and deployment, showing the features of simple structure, light weight, and low impact [21–24], etc. The deployable structures have developed diverse space deployable components with large deployment/fold ratio, including hinge, beam, truss, antenna and solar array [25–27]. For example, Santo et al. shown the feasibility of shape memory epoxy foams for building multi-functional composite structures on the International

* Corresponding author at: Centre for Composite Materials and Structures, Harbin Institute of Technology (HIT), No. 2 YiKuang Street, PO Box 3011, Harbin 150080, People's Republic of China.
E-mail address: lengjs@hit.edu.cn (J. Leng).

https://doi.org/10.1016/j.compstruct.2018.08.041
Received 1 April 2018; Received in revised form 25 June 2018; Accepted 14 August 2018
Available online 17 August 2018
0263-8223/

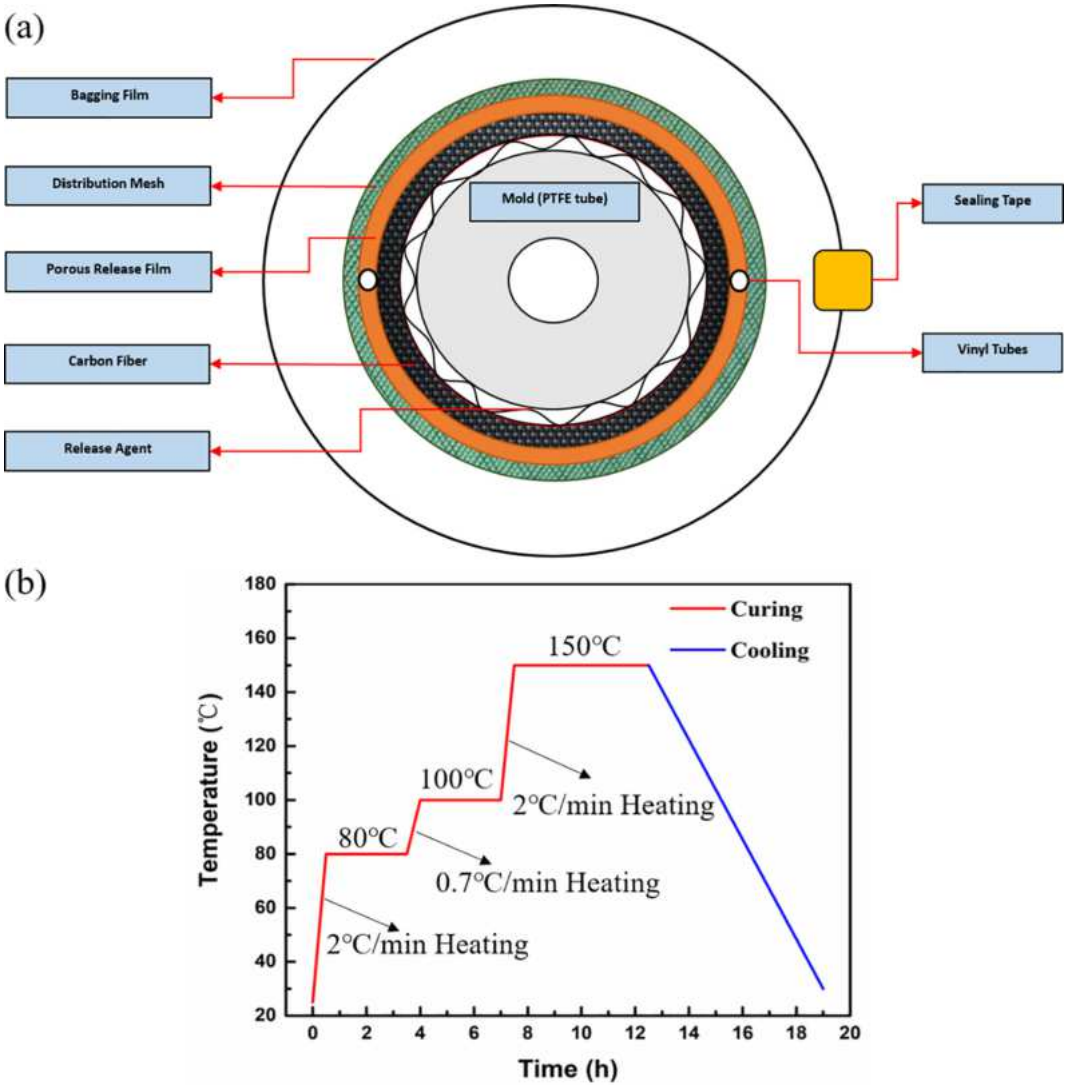

Fig. 1. (a) Schematic illustration of modified VARTM process and (b) the curing cycle of SMPC tube.

Space Station and found that the recovery ability could not be affected by the micro-gravity environment [28]. In 2013, during the BION-M1 mission of the Soyuz spacecraft 180° folded SMPC laminate was observed to deploy, which provided important evidence for designing self-deployable structures [29]. Typically, hinges are the most extensively used driven components during the deployment process of deployable structures. Elastic Memory Composite (EMC) materials developed by Composite Technology Development, Inc. was designed into hinges to deploy an experimental solar array on the TacSat-2 Mission in 2006 for the first time [30]. AEC-Able Engineering Co. studied a Coilable Longeron for deployable boom, which could be bent to a helix for packaging and deploy with the force generated from the storage stain energy of the longerons [31]. Yee et al. proposed a kind of carbon fiber reinforced plastic tape springs, which were investigated by the nonlinear finite-element analysis method in detail [32]. Leng et al. designed a SMPC hinge with the purpose of actuating a prototype of a solar array, and implemented the whole deployment time of 80 s and deployment ratio of approximately 100% during the recovery process [33]. Soykasap investigated the folded configuration of woven carbon fiber reinforced plastic composite sheets with maximum strain and Tsai–Wu failure criteria [34]. Ahn et al. demonstrated the manufacturing method of deployable structures made of smart materials based actuators, which had the capability of continuous morphing [35]. Generally, hinges based on SMPC are assembled by a pair of symmetrical SMPC laminates and two connecting structures on both sides combining SMPC laminates and structures to actuate. Hinges with larger distance between SMPC laminates possess higher stiffness, but more buckling deformation in the bending process [36–39], which result in easily damage of the material. On the contrary, the stiffness of SMPC hinge would be reduced with small distance between laminates.

In this work, a new type of deployable structure based on carbon fiber reinforced shape memory epoxy composites is developed. The deployment part consists of two symmetrical arc-shaped laminates, which is obtained from a whole SPMC tube. The novel deployable structure, which is structural and functional integration without assembling process, possesses improved reliability and performance, self-locking and self-deployable, more controlled deployment process and higher post-deployment stiffness and strength when compared to general SMPC hinges. Three point bending tests under different temperatures and modal tests have been conducted, in order to demonstrate the variable stiffness and mechanical properties of the deployable structure. Meanwhile, shape memory recovery tests, including the integrative SMPC hinge and a whole deployable structure, have been performed to investigate the shape memory effect. The experimental results and computational results are compared for further illustration and verification.

Fig. 2. Fabrication process of SMPC tube.

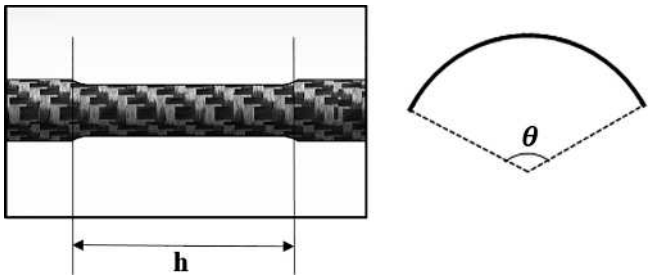

Fig. 3. Dimensions of arc-shaped laminates.

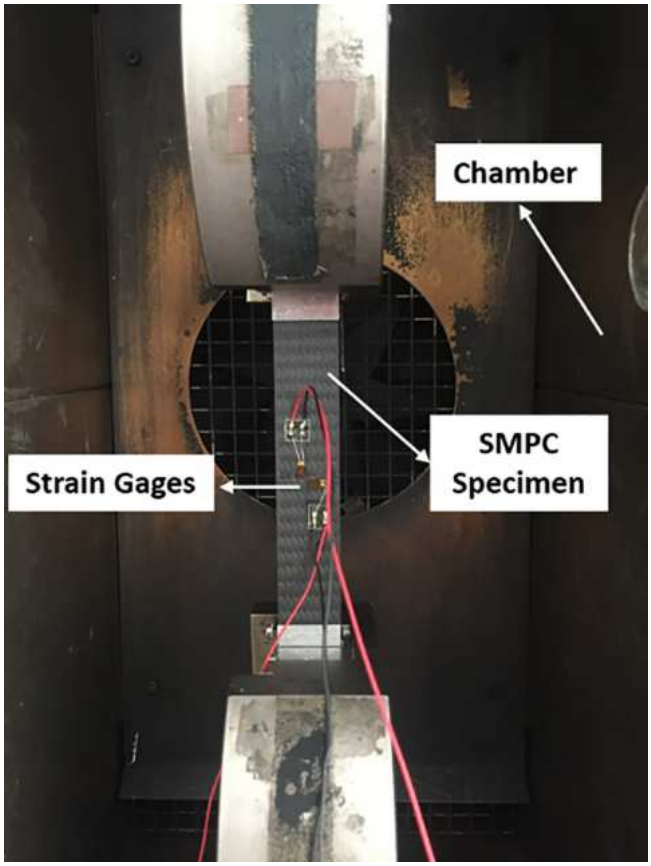

Fig. 5. Tensile experiment of SMPC.

2. Design and fabrication of integrative SMPC hinge

In this study, the SMP material adopted was epoxy-based shape memory resin developed by Jinsong Leng's group [24], of which the glass transition was 100 °C. The Carbon fiber (T300-3K, plain weave) reinforced shape memory composite tube was fabricated by vacuum assisted resin transfer molding (VARTM) that was modified for cylinder, as illustrated in Fig. 1(a). To overcome the difficulty of demolding for a relatively long product in fabrication process, a special design of the mold was particularly important. Polytetrafluoroethylene (PTFE) tube was selected as mold because of the smooth surface, which made it easy to demold, and the melting point of 327 °C, which insured that it could work effectively during the curing process. The PTFE mold was cleaned with acetone, followed by Freekote. The carbon fiber sheets in the predetermined configuration (± 45° along the axis) were winded on the mold, and then covered by porous release film and distribution

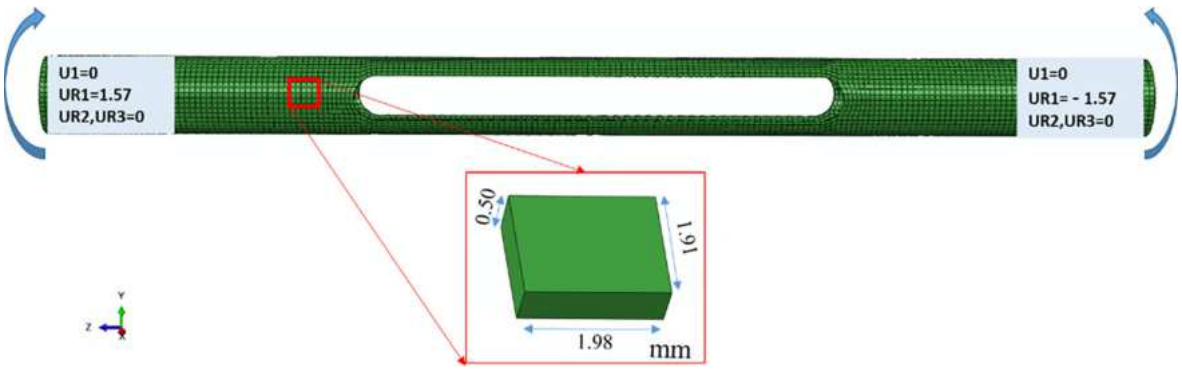

Fig. 4. Finite element model of an integrative SMPC hinge.

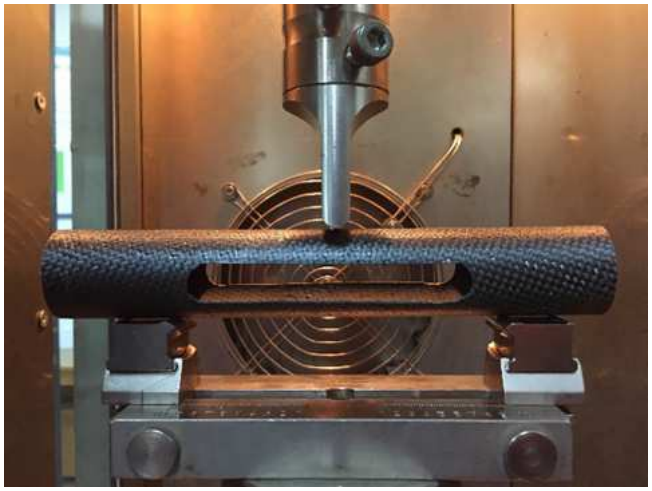

Fig. 6. Three point bending tests of integarative SMPC hinge.

mesh as shown in Fig. 2. After the preparation process, the setup was vacuumed for at least 1 h to make sure there was on air in the system. Fig. 1(b) illustrated the detailed curing process, which was at 80° for 3 h, 100° for 3 h and 150° for 5 h. The SMPC tube specimen was fabricated with the length of 1500 mm, an inner diameter of 25 mm and an outer diameter of 28 mm.

The SMPC tube was cut into two symmetrical arc-shaped laminates with the length of 100 mm and the arc angle of 120° in the bending area, which made it possible for the SMPC tube to be packaged as a whole structure. The relevant characteristics of the integrative SMPC hinges are shown in Fig. 3. The arc angle θ is closely related to the shape memory deformation of the arc-shaped laminates. The laminates would be more stable and provide larger restoring moment with a bigger arc angle. However, with the growth of the arc angle, deformation of the side edges of arc-shaped laminates would markedly increase, thus leading to further damage of the material. The experimental results show that arc laminates with the arc angle of 120° could meet the requirements of design parameters, which could also maintain no damage with bending radius of 20 mm. This strategy offers several advantages. The function of these two symmetrical arc-shaped laminates is to provide very high stiffness when deployed, and accommodate very high strains when folded like a pair of hinges. Meanwhile, they show obvious superiority of light weight and structure integration without complex mechanical connections.

3. Computational model analysis

3.1. Bending property analysis of integrative SMPC hinge

The distributions of stress and deformation with different bending angles under the influence of temperature were predicted using the finite element analysis (FEA) software ABAQUS. A finite element model was created to simplify the integrative hinges with inner diameter of 25 mm, outer diameter of 28 mm, length of 400 mm, h = 100 mm and $\theta = 120°$ (shown in Fig. 3). The hinge was meshed using C3D8R elements, the number of which was 23568. The mesh technique selected was 'Structured' and the boundary conditions applied were on both ends of the hinge, as shown in Fig. 4. The step Visco was used to simulate the deformation of integrative hinge. The material model was established based on previous work [40] in Prof. Jinsong Leng's group. The material parameters (thermal expansion coefficient, coefficient C1, C2, and viscoelastic parameters) were chosen from the literature [41] related to similar shape memory epoxy system. The elastic modulus of the material at different temperatures were obtained from the tensile tests.

3.2. Modal analysis of different hinge types

In order to conduct the modal analysis of SMPC tube, integrative SMPC hinges and traditional SMPC hinges [33], the FEA software ABAQUS was adopted with finite element method. The step Frequency in liner perturbation was selected. The element type was C3D8R and mesh technique was 'Structured'. The free boundary condition maintained the same as modal testing in order to compare with each other. The whole SMPC tube (with the length of 1500 mm, an inner diameter of 25 mm and an outer diameter of 28 mm), SMPC tube with integrative hinges described in Fig. 3, and SMPC tube connected with traditional SMPC hinges, the length and arc angle of which are the same as integrative hinges, were investigated, which were named type I, type II, and type III respectively. The material properties of SMPC at 25 °C were

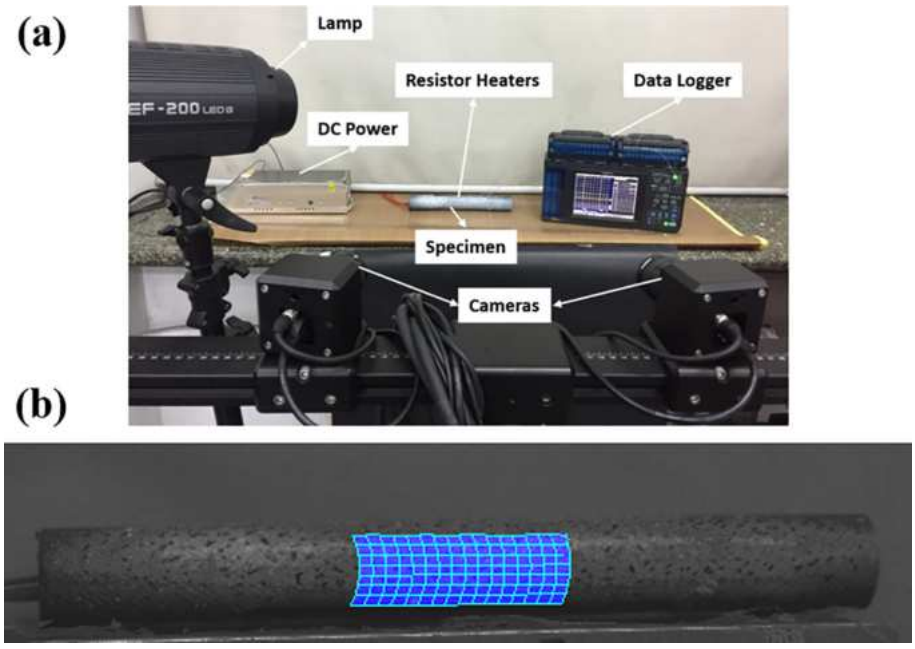

Fig. 7. DIC setup (a) and specimen (b) for calculation.

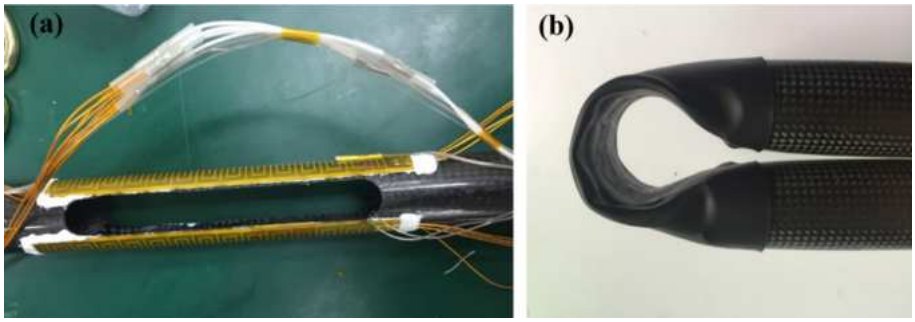

Fig. 8. Distribution of resistor heaters (a) and bent integrative SMPC hinge covered with shrinkable tube (b).

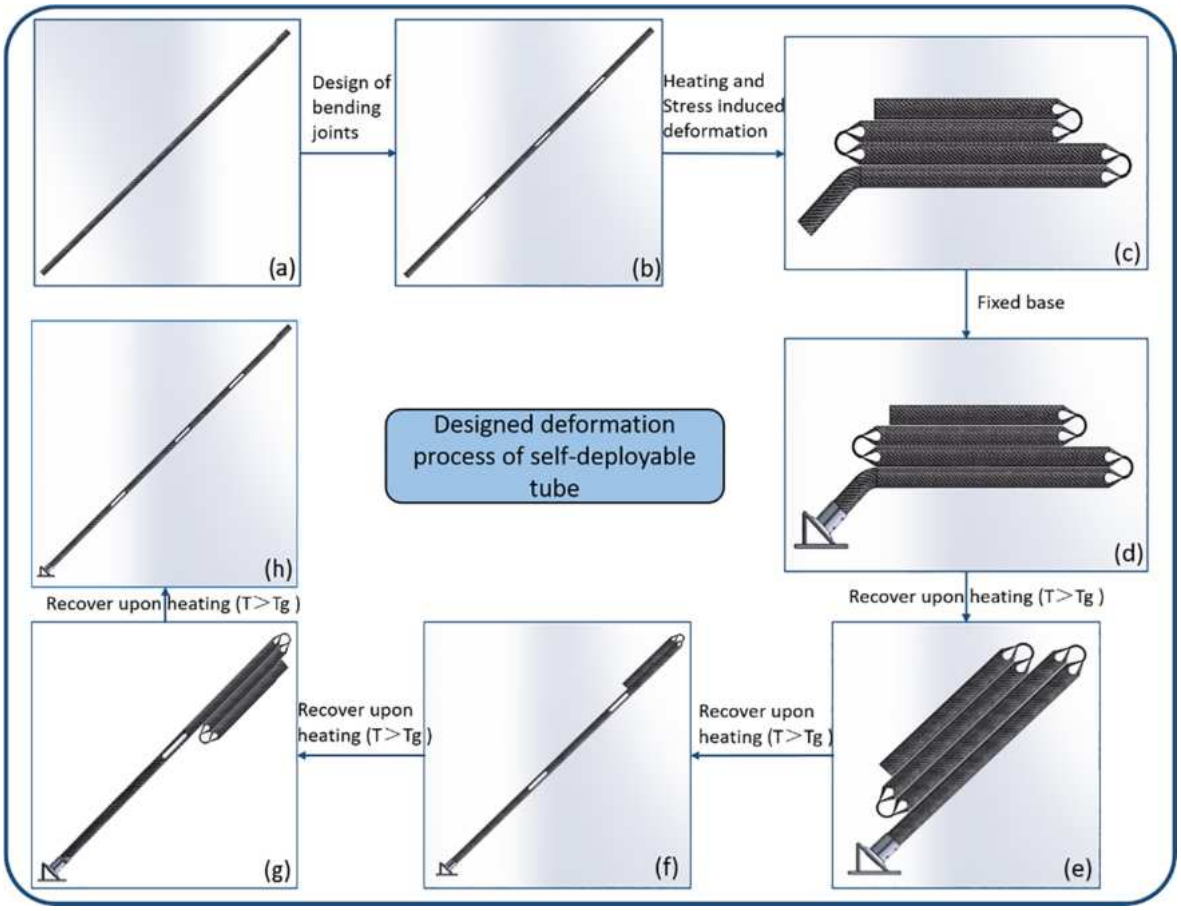

Fig. 9. Designed deformation process of self-deployable structure.

from the tensile tests, and the material type of the connection parts between SMPC hinge and tube in traditional SMPC hinge were defined as aluminum alloy (Elasticity modulus E = 72 GPa Poisson's ratio v = 0.3), which is the same as the material parameters selected in the real structure.

4. Experiments

4.1. Dynamic mechanical analysis

The basic properties of pure shape memory epoxy play a significant part in the performances of SMPC and SMPC based structures. In order to conduct thermo-mechanical analysis of pure SMP, a dynamic mechanical analyzer (NETZSCH DMA Q800) was adopted to identify the storage modulus and tangent delta. Sample with dimensions of $30 \times 5 \times 1.2\,mm^3$ were tested at 5 Hz and at a heating rate of 5 °C/min from 25 °C to 150 °C. The glass transition temperature (Tg) of SMP was determined at the peak value of tangent delta.

4.2. Static mechanical tests

Static mechanical tests were conducted with the temperature controlled from 25 °C to 125 °C with an increment of 25 °C. A thermal regulating chamber was applied to create a controlled conditions with specific temperature, while INSTRON 5569 with 50 KN load cell (for tensile tests) and ZWICK/Z010 with 1 kN load cell (for three point bending tests) were adopted to obtain a constant loading rate of 2 mm/min, as shown in Figs. 5 and 6.

4.2.1. Tensile experiments of SMPC

Tensile experiments of SMPC specimens have been carried out under different temperatures (25 °C, 50 °C, 75 °C, 100 °C, 125 °C) for a

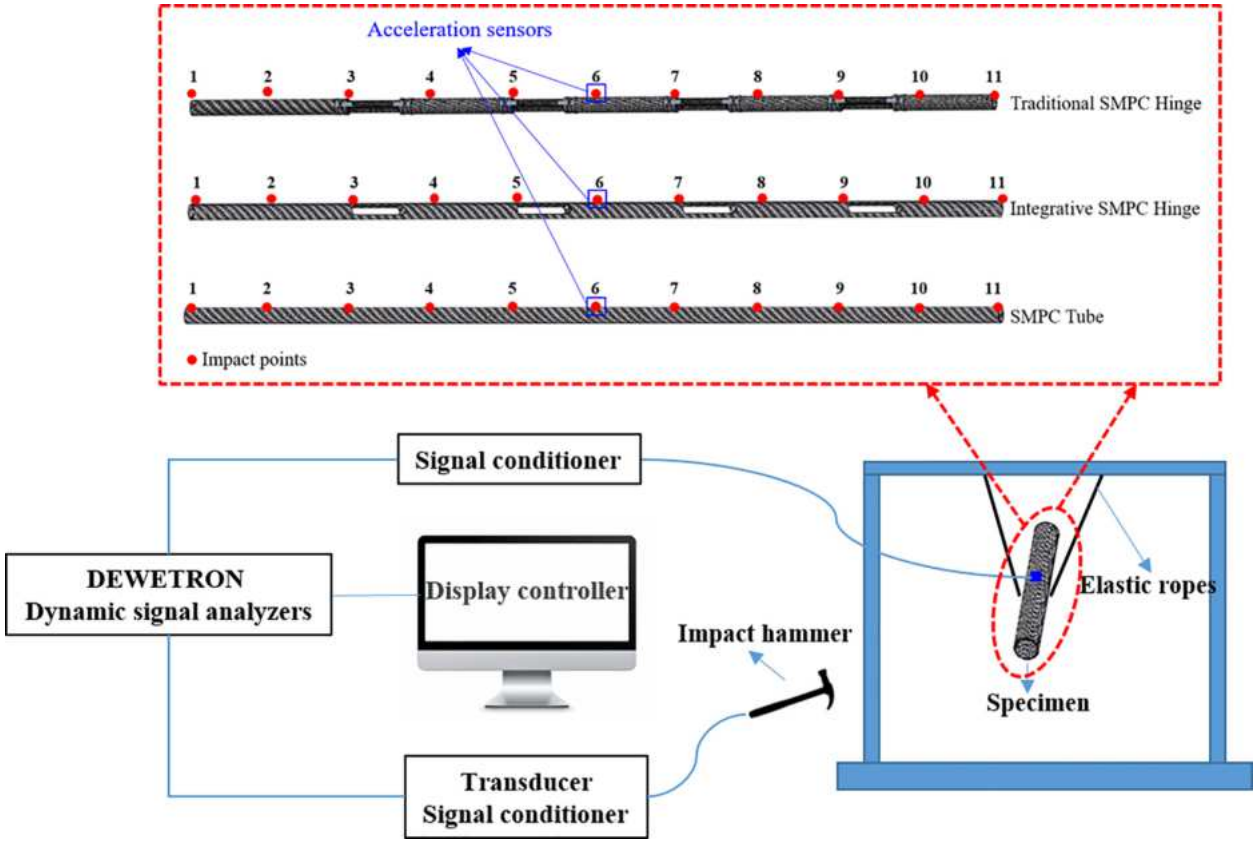

Fig. 10. The experimental equipment of modal testing and arrangement of impact points and response points on specimens.

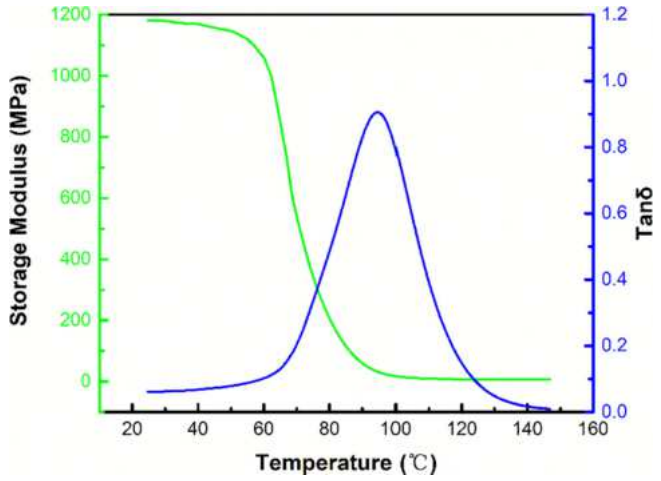

Fig. 11. Storage modulus and tangent delta versus temperature of pure SMP.

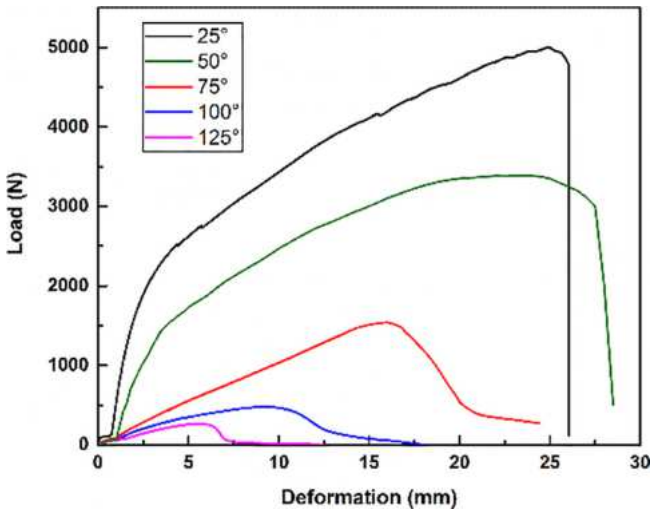

Fig. 12. Deformation-load curves of SMPC under different temperatures from tensile tests.

better understanding of the material adopted in integrative SMPC hinges, from which the temperature dependent mechanical properties including elastic modulus and strength were determined. Fracture morphologies and temperature sensitivity of SMPCs were observed and analyzed. Three specimens with 250 mm × 25 mm × 1.5 mm according to ASTM D3039 were tested at each temperature. The applied force, displacement and strain were recorded.

4.2.2. Three point bending tests of integrative SMPC hinge

It is necessary to verify the variation of stiffness of integrative SMPC hinge under different temperatures to investigate the bending performance. The experiments at each temperature (25 °C, 50 °C, 75 °C, 100 °C, 125 °C) were performed on three specimens, the dimensions of which were with inner diameter of 25 mm, outer diameter of 28 mm, length of 200 mm, h = 100 mm and θ = 120° (shown in Fig. 3). The span length was 120 mm in the bending tests. The tests stopped when the displacement of point in the central span reached the maximum value of 10 mm. During the bending test process, the values of applied force and displacement were recorded.

4.3. Digital image correlation measurements

To investigate the displacement and strain field of integrative SMPC hinge during the bending process, digital image correlation (DIC)

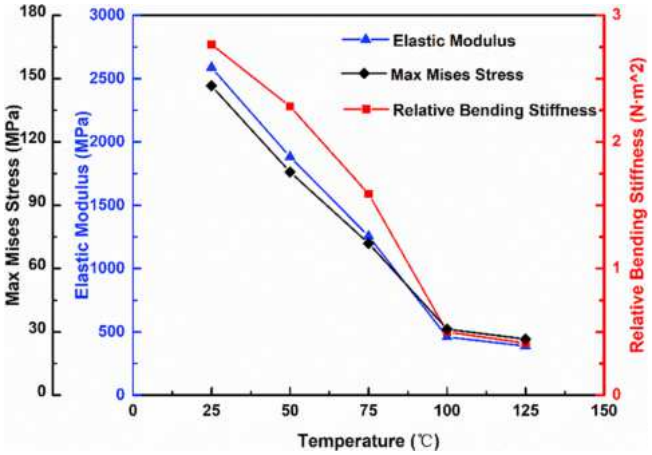

Fig. 13. Curves of elastic modulus (from tensile tests), relative stiffness (from three point bending tests) and max Von Mises stress (from ABAQUS simulation) versus temperature.

technique was applied for measurements, which compared the deformed images with the first image (set as reference image) for calculation. As shown in Fig. 7, two cameras with resolution of 2448 × 2048 pixels and lens of 25 mm were utilized to collect images of bending surface at frequency of 5 Hz, and a lamp was to improve the brightness. Two resistor heaters (resistance R = 29 Ω) powered by DC power supply (voltage V = 23 v) provided heat for deformation from 0° to 180° of integrative SMPC hinge. The specimens had white background with random black speckles for contrast, which were applied by white and black spray paint. The temperature of bending area was monitored by Hioki MEMORY HiLOGGER LR8400 portable data logger. The effective view field was approximately 20 mm × 40 mm due to the limit of large angle deformation.

4.4. Shape memory recovery tests of integrative SMPC hinge

In order to actuate the SMPC tube with heat, resistor heaters (resistance R = 29 Ω) were stuck on the outside surfaces of the symmetrical arc-shaped laminates in bending areas, as shown in Fig. 8. Shrinkable tubes were adopted to cover the outside surface for the purpose of protecting the wires of resistor heaters, as shown in Fig. 8. Hioki MEMORY HiLOGGER LR8400 was adopted to measure the temperature of the hinge surface in heated area.

The self-deployable structure consists of a SMPC tube with three integrative hinges, two resistor heaters for each deformation hinges and a base with a 45° angle providing support for the tube fixing. The designed deformation process of self-deployable structure, of which two configurations are demonstrated, the folded configuration and the deployed configuration, are shown in Fig. 9. The SMPC tube was bent into five parts with three 180° angle deformation integrative hinges and one

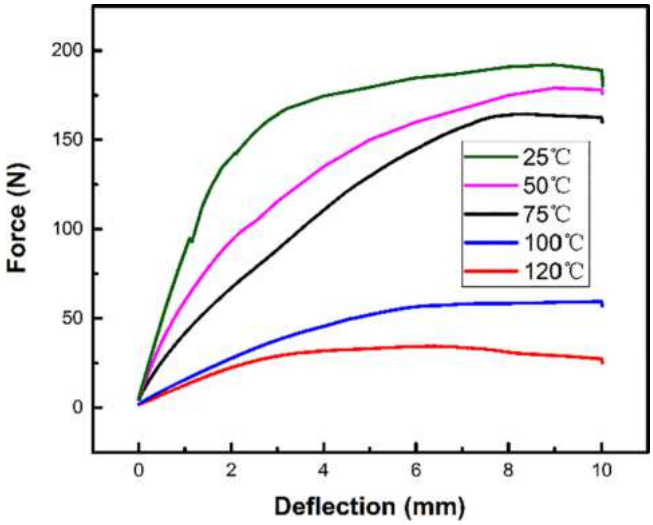

Fig. 15. Experimental curves of applied force versus deflection.

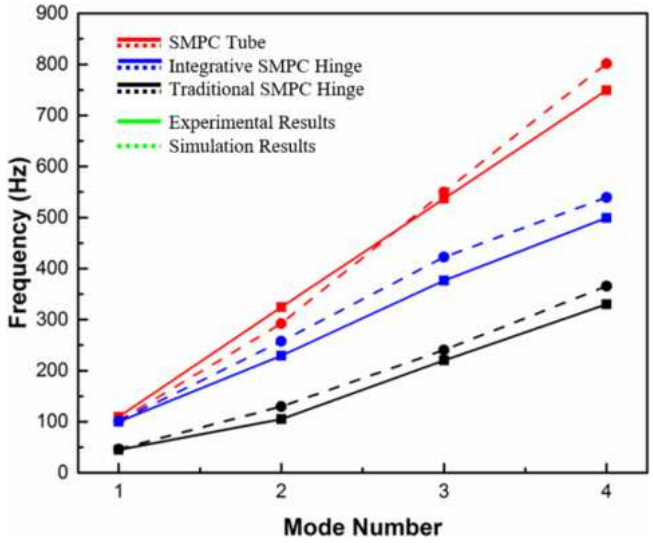

Fig. 16. Comparison of natural frequencies of experimental and simulation results.

45° angle deformation hinge by heat-treatment, which provided driving force for recovery process. Then, a base was assembled to one end of the SMPC tube so that it is convenient to make the SMPC tube fixed. At this point, the folded configuration of self-deployable structure is obtained. For shape memory recovery process, the folded self-deployable tube are heated in sequence from the end with base to the other, deforming to the original state under control.

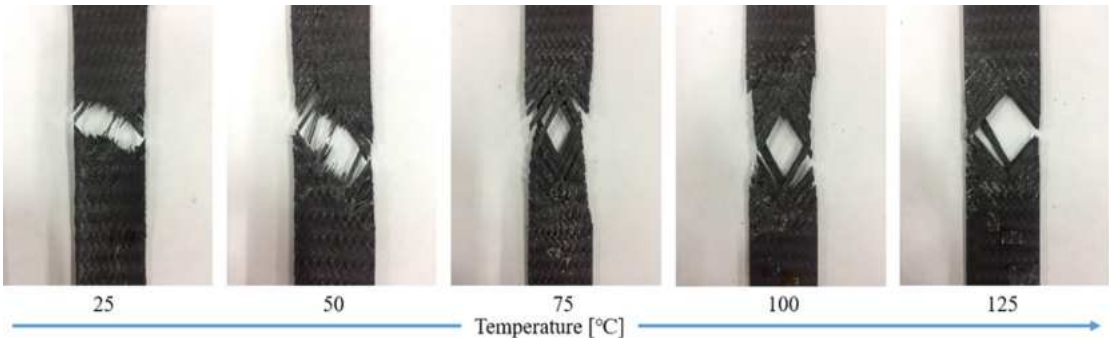

Fig. 14. Fracture morphology of SMPC under five different temperatures.

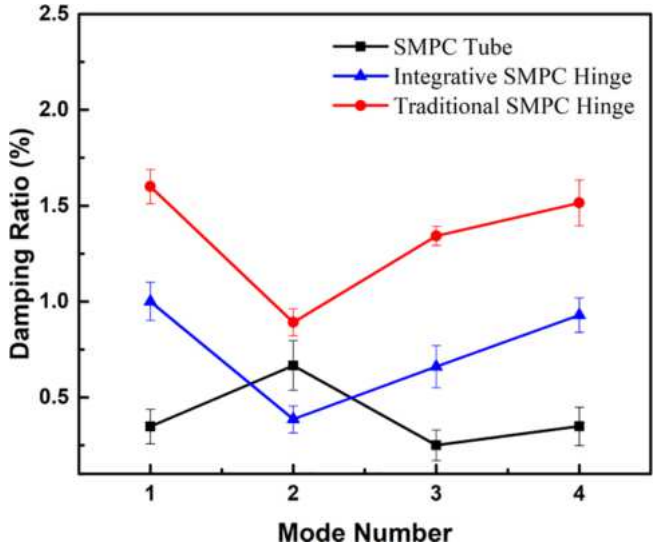

Fig. 17. Comparison of damping ratios for three types of structures.

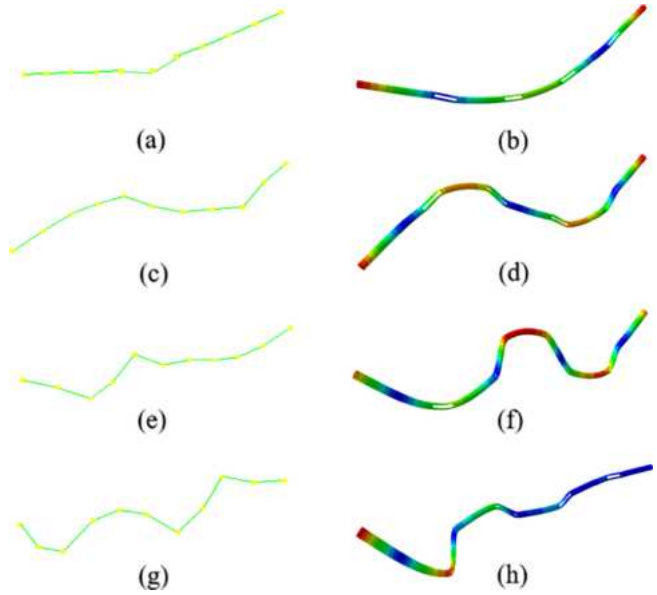

Fig. 18. The first four mode shapes of integrative SMPC hinge from experimental (a, c, e, g) and simulation (b, d, f, h) results.

4.5. Modal testing of different hinge types

In order to investigate the effect of different hinge types on structural mechanical property, model tests were designed and performed through hammering impact method. The three types of structures (type I, type II, and type III) have been prepared. The arrangements of impact points and response points are shown in Fig. 10, where 11 impact points are set along the axial direction of SMPC tube with even distribution and the response point is arranged at the 6th point. The specimens were suspended on a designed holder by light elastic ropes with the purpose of simulating the free boundary conditions. Impact hammer with model SN30979 and sensitivity 12.25 mV/N was applied to provide excitations, and acceleration sensor with model SN46550 and sensitivity 10.07 mV/m/s^2 was to detect vibration responses simultaneously. The impact points are excited five times to guarantee consistent data, during which coherence function is the reference standard used to evaluate their reliability. As shown in Fig. 10, the impact signal and response signal were collected and processed by DEWETRON dynamic signal analyzer, where the modal parameters including natural frequencies, mode shapes and damping ratios were obtained with the Fast Fourier Transform (FFT) analyzer, Frequency Response Function (FRF) Geometry and modal circle fit method [42,43]. Force window was used to eliminate the noises that may appear on the impact excitation channel. At the same time, the exponential window was employed for hammer signals to meet the requirements of FFT.

5. Results and discussion

5.1. Dynamic mechanical properties of pure SMP

The storage modulus and tan δ of pure shape memory epoxy as a function of temperature are reported in Fig. 11. Tan δ presents the ratio of loss modulus to storage modulus, the peak value of which is defined as Tg. Therefore, the Tg value of pure SMP is about 98 °C. It could be observed that there is a sharp decrease in storage modulus within the glass transition region, illustrating the two different states at varying temperatures in SMP, namely glassy state and rubbery state. The glass transition process occurs in the region between these two states, which is important for shape memory material.

5.2. The effect of temperature on SMPC

The curves of load versus displacement from tensile tests are shown in Fig. 12. The fracture strength of SMPC declines obviously with the increase of temperature, which are from 138 MPa at 25 °C, 15 MPa at 100 °C (Tg), to 10 MPa at 125 °C. Fig. 13 illustrates that the elastic modulus is 2588 MPa at 25 °C, dropping to 459 MPa at 100 °C and 388 MPa at 125 °C, the reason behind which is that the SMP transfers from the glassy state to rubber state gradually when external environment changes from room temperature to Tg temperature, and then maintains in rubber state when temperature is in 100–125 °C. Fig. 14 shows the fracture morphology of tensile tested SMPC under different temperatures. Specimens at 25 °C have straight fractures, but the fractures of specimens at 50 °C become oblique, and obvious breaks of carbon fibers could be observed at both 25 °C and 50 °C, which means the epoxy and carbon fibers possess strong interfacial adhesion force. It could be found that the fracture pattern turns to fiber pull-out above 75 °C due to the rubber state of shape memory epoxy and the pull-out is easier at higher temperature. The interfacial strength between epoxy and carbon fibers, which decreases with the increase of temperature, plays a significant role in fracture patterns during fracture process of the composites.

5.3. Mechanical properties of integrative SMPC hinge

5.3.1. Variable stiffness

The three point bending experiment curves of applied load versus displacement under different temperatures are described in Fig. 15. The integrative SMPC hinge shows typical properties of elastic material at room temperature. Elastic deformation happens at initial stage, followed by inhomogeneous yield plastic deformation and homogeneous plastic deformation. The integrative SMPC hinge processes large extensibility with the influence of heat, which results from the intrinsic elastic networks of shape memory epoxy. The relative bending stiffness EI of integrative SMPC hinge is expressed via:

$$\mathrm{E} = \frac{l^3}{48I}\left(\frac{\Delta F}{\Delta \delta}\right)$$

where l is the span length, ΔF is the applied load and $\Delta\delta$ is the deflection of central point in span. And $\Delta F/\Delta\delta$ can be calculated according to the slope of initial linear stage in the curves obtained at different temperatures. The tendency of bending stiffness based on temperature is illustrated in Fig. 11. The bending stiffness is 2.81 N m^2 at 25 °C, followed by 2.28 N m^2, 1.59 N m^2, 0.5 N m^2 and 0.41 N m^2, at 25 °C, 50 °C, 75 °C, 100 °C and 125 °C respectively. The elastic modulus of

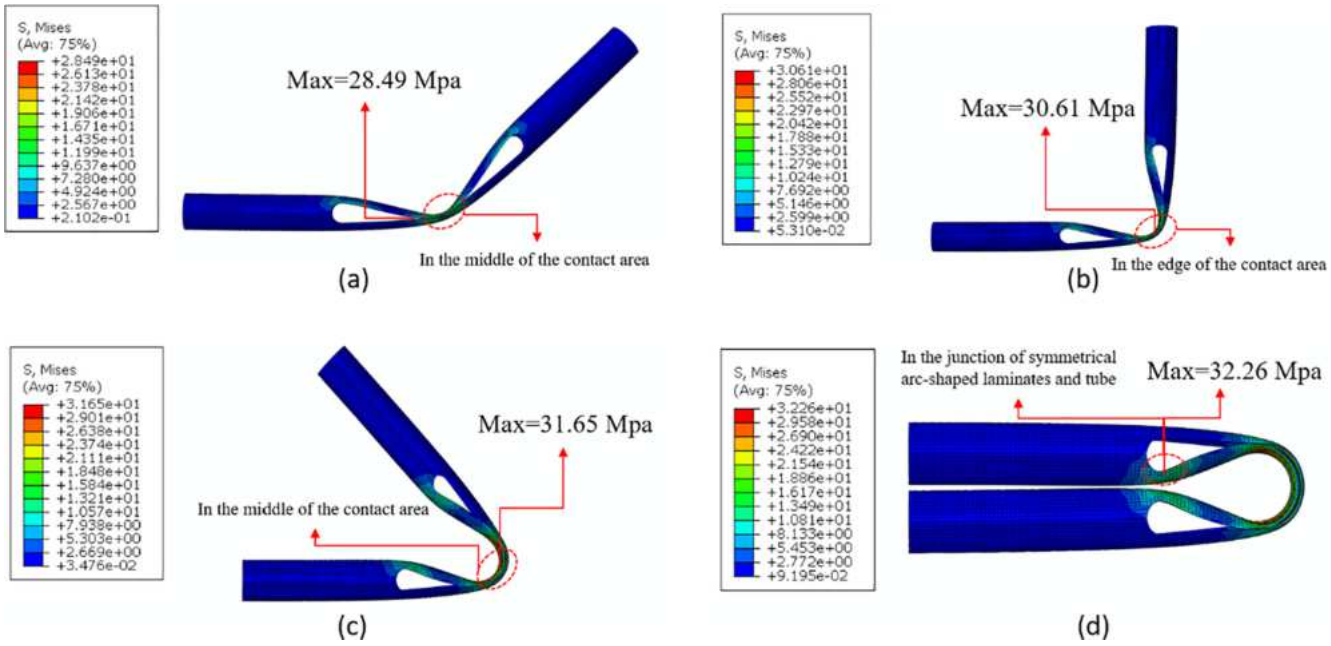

Fig. 19. Mises stress distribution of integrative SMPC hinges bent with 45° (a), 90° (b), 135° (c), and 180° (d).

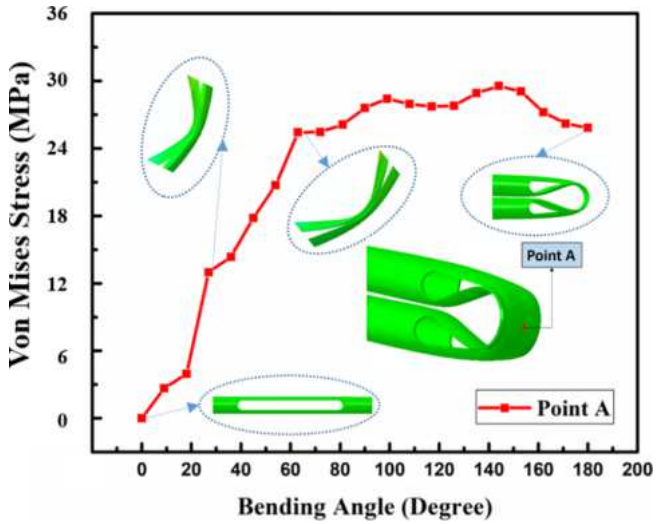

Fig. 20. The Von Mises stress versus bending angle of Point A.

shape memory epoxy decreases dramatically under temperature near Tg, because of which the stiffness has a steep drop when temperature rises from 75 °C to 100 °C. The sight decrease of elastic modulus of shape memory epoxy under temperature over Tg leads to a relatively slow drop of stiffness from 100 °C to 125 °C. The value of bending stiffness at 25 °C shows a nearly sevenfold increase, compared to the figure at 125 °C. The integrative SMPC hinge possesses the characteristic of variable stiffness owing to the temperature change.

5.3.2. Modal characteristics

The first four order natural frequencies and mode shapes obtained from the finite element method are shown in Figs. 16 and 18. Comparisons were made between the results from simulation and experiment.

Fig. 16 reports that the natural frequencies of integrative SMPC hinges and traditional SMPC hinges presents decline trends in varying degrees, resulting from the existence of two hinge forms. Compared with traditional SMPC hinges, integrative SMPC hinges possess much higher natural frequencies, which means that integrative SMPC hinges can significantly improve structural total stiffness without complex mechanical connections. There is no obvious difference in amplitude peaks in frequency response function of the three types of structures, implying little structural damping variation among the three types of structures. Comparisons of natural frequencies of three kinds of specimens obtained from experimental and simulation results are illustrated in Fig. 16. Results from experiments are demonstrated with solid lines, while these from simulation are shown with dash lines. And the color red, blue and black present SMPC tube, integrative SMPC hinges and traditional SMPC hinges, respectively. It can be observed that the experimental data show good consistency with the simulation data, verifying the feasibility and applicability of the methods. The maximum relative error of the first four orders between experimental and simulation results is about 6%, which is acceptable and inevitable, due to the experimental errors and fabrication defects. It is obviously that the natural frequencies of SMPC tube are located in the upper part of the other type specimens, because of the higher stiffness of the whole SMPC tube. The first four order damping ratios of three types of structures from experiments are shown in Fig. 17, which are determined by using modal circle fit method [42]. The ranges of damping ratios for three types of structures are from 0.25% to 1.60%. It can be observed that the traditional SMPC hinges possess higher damping ratio than SMPC tube and integrative SMPC hinge, the reason behind which is that the connection parts in traditional SMPC hinges increase the internal friction of the structure, and have the ability of absorption of vibration. As shown in Fig. 18, the first four order mode shapes of integrative SMPC hinges from both modal tests and finite element simulation are compared. The mode shapes from two kinds of results are basically in agreement. It can also be found that the large ratio of length and radius brings about most longitudinal mode shapes in first four orders.

5.3.3. Bending properties

In order to investigate flexural properties, the hinge was bent into 180°, during which Mises stresses at four different angles (45°, 90°, 135°, and 180°) were studied. Here laminate 1 referred to the laminate on stretch side, while laminate 2 referred to the laminate on compression side. Fig. 19 demonstrates the simulation results at 100 °C. The location distribution of maximum Mises stress with different bending angles were not the same. As shown in Fig. 19, the maximum Mises stress located right in the middle of inner surface of laminate 1 when

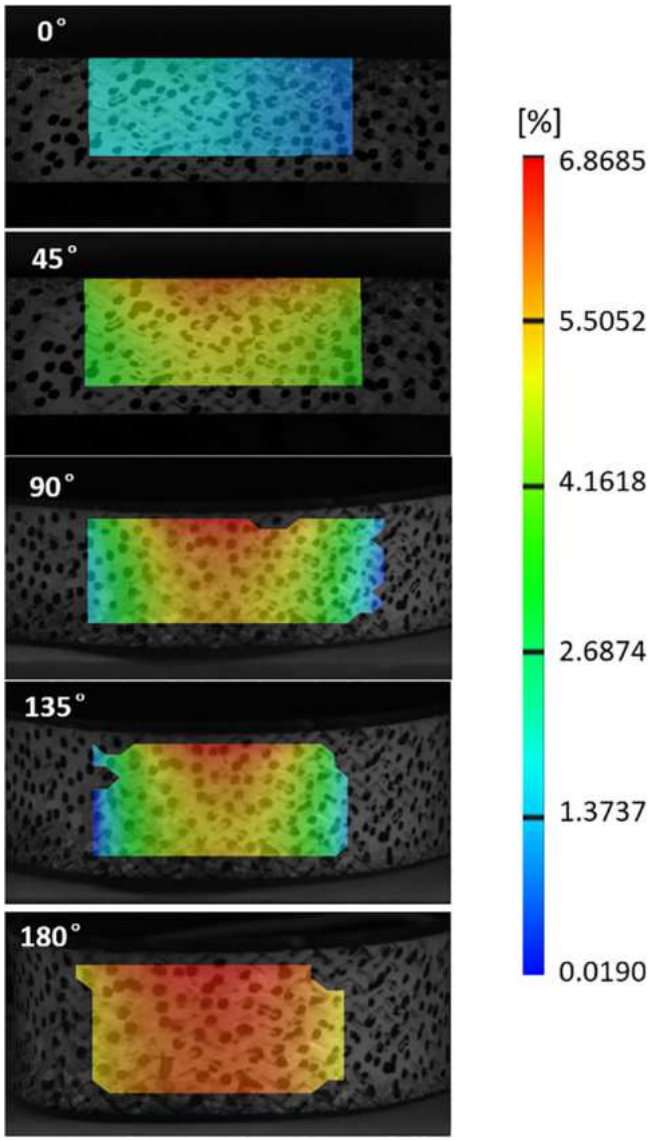

Fig. 21. Surface strain distribution in deformation process at 100 °C.

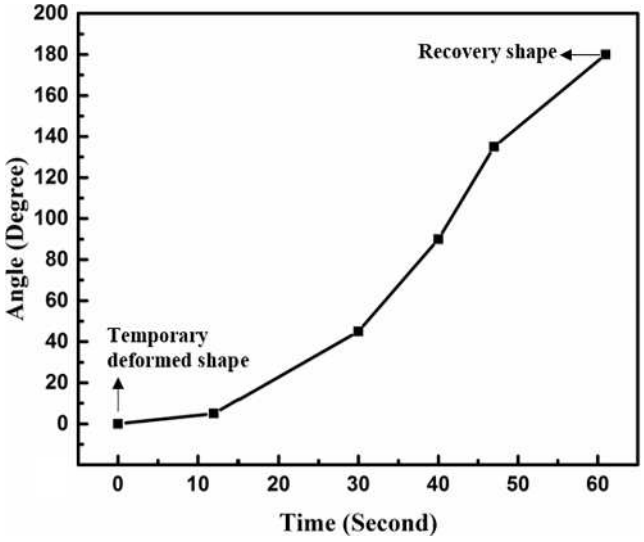

Fig. 23. Relationship of recovery angle and time of a single integrative SMPC hinge.

the hinge was bent with 45° and 135°. While the hinge was bent with 90° and 180°, the maximum Mises stress located respectively in the edge of inner surface in middle bending area and the junctions of symmetrical arc-shaped laminates and tube. Although the locations differed from each other, the value of maximum Mises stress raised with the increasing of bending angle, which were 28.49 MPa, 30.61 MPa, 31.65 MPa, and 32.26 MPa, respectively.

The middle point of bending area in outside surface of laminate 1, named Point A, drew particular interests and was given special attention, due to the fact that Point A had maximum tensile deformation during the bending process. The relationship between Mises stress of the point and bending angles was recorded from ABAQUS simulation, as shown in Fig. 20. The Mises stress of Point A increased steadily with the growth of bending angle, during which the maximum Mises stress was 30.2 MPa at the bending angle of 144°. The stress increased sharply to a relative high value when the hinge was bent to 27°. The reason behind this is the contact of two laminates, which led to a rapid increase of Mises stress during the bending process. When the hinge continued to be bent to a larger angle, the Mises stress rose to 25.5 MPa

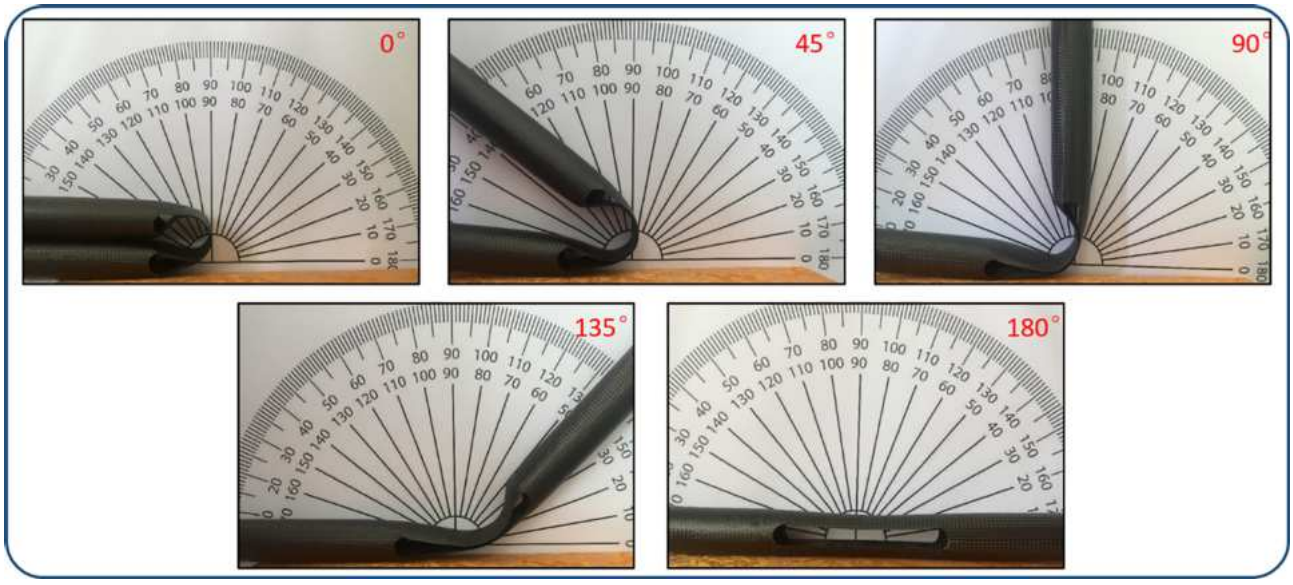

Fig. 22. Bending recovery process of a single integrative SMPC hinge.

Fig. 24. Shape memory recovery process of self-deployable structure.

Table 1
Characteristics during the shape memory recovery process.

Characteristics	The 1st hinge	The 2nd hinge	The 3rd hinge	The 4th hinge
Driving power	18 w	18 w	18 w	18 w
Recovery time	30 s	60 s	58 s	56 s
Maximum temperature	110 °C	113 °C	109 °C	108 °C

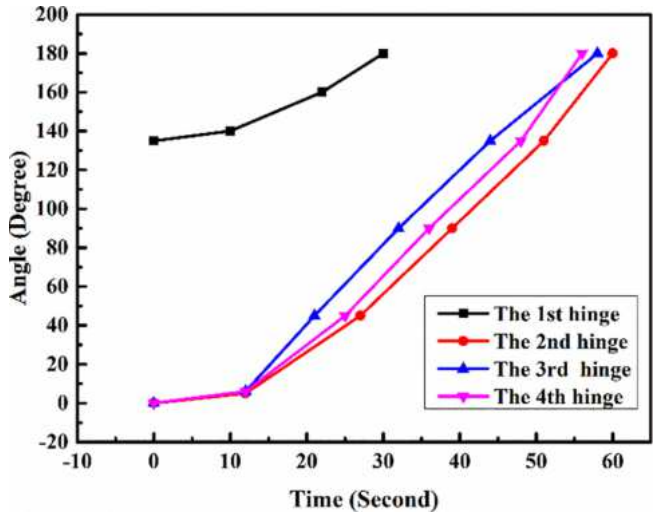

Fig. 25. Relationship between recovery angle and time of self-deployable structure.

at 63°, reflecting the full contact process of two laminates.

The relationship between maximum Von Mises stress and temperature during bending process from 0° to 180° is shown in Fig. 13. It is obvious that the max Mises stresses of integrative SMPC hinge show a rapid decline from 25 °C to 100 °C, and the downward trend becomes quite slow from 100 °C to 125 °C, resulting from the change of elastic modulus. This tendency provides a basis for selection of appropriate temperature to deform the target shape of integrative SMPC hinge. Fig. 21 demonstrates the strain distribution of tension sides in deformation process at 100 °C from DIC results. It can be seen that the strain concentrations display in central areas, which corresponds to the stress concentrations. The area of strain concentrations is wider under larger bending angle. The strain values have deviations (maximum relative errors of 1.8% at 45°) when compared with simulation results, which is caused by experimental errors and simulation accuracy. However, the strain distribution and tendency obtained from DIC measurements are consistent with ABAQUS computational data. The missing areas of stain fields at 90°, 135° and 180° result from the loss of collection points at large bending angles.

5.4. Shape memory properties of integrative SMPC hinge

5.4.1. Integrative SMPC hinge

Fig. 22 shows the detailed bending recovery process of a single integrative SMPC hinge. Relationship of recovery angle and time is shown in Fig. 23. It took 30 s to recover to 45°, 40 s to 90°, 47 s to 135°, and 61 s to 180°. The shape memory recovery speed of the integrative SMPC hinge is relative high during the recovery process from 45° to 135°, due to the fact that there are adequate heat and storage energy for recovery in the middle stage. The shape recovery ratio maintains 100% with 10 times fold-deploy process.

5.4.2. Deployable structure

The folded configuration of self-deployable structure after heating and stress induced deformation is demonstrated in Fig. 24. The packaged SMPC tube was heated in a predetermined sequence and deployed. The characteristics during the recovery process are shown in detail in Table 1. It took 30 s for the first hinge (45° angle deformation) to recover to the original shape. As for the next three hinges (180° angle deformation), a little longer time about 60 s was used to finish deformation recovery. The recovery time can be adjusted to meet different requirements through altering the actuation power. From the relationship between bending angle and recovery time (Fig. 25), several rules could be found out. Approximate 12 s were needed to preheat bending area to approach to glass transition temperature (Tg) of the shape memory polymer composites, then obvious deformation recovery was triggered. The fastest recovery stage was from 45° to 135° for one hinge, which was approximate 18 s except for the effect of gravity. During this period, the bending area was fully heating up to Tg and

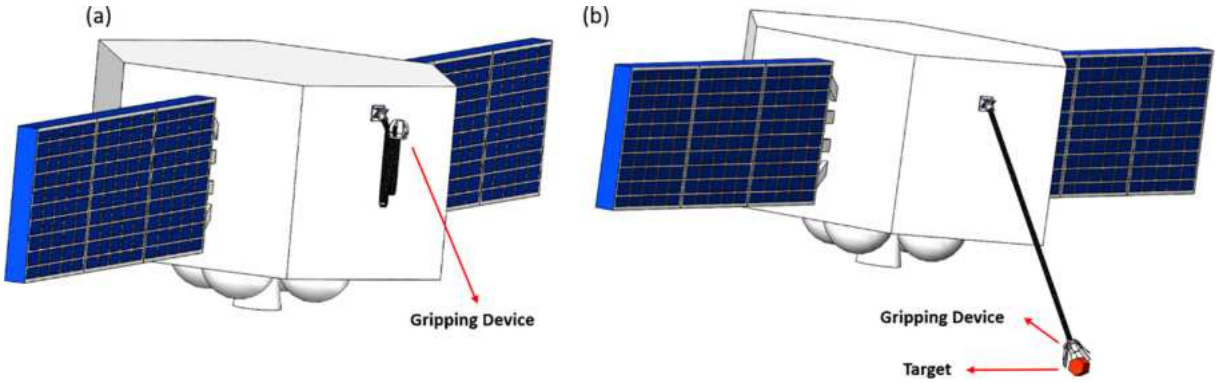

Fig. 26. Prospective self-driven gripping device (a) folded configuration (b) deployed configuration.

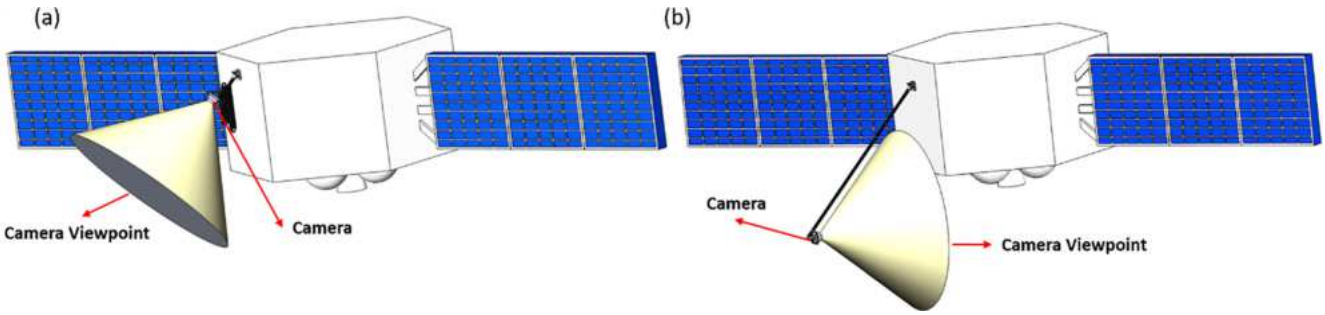

Fig. 27. Prospective multi-angle imaging system (a) folded configuration (b) deployed configuration.

stored enough shape memory potential energy to release. The recovery rate was faster when the direction of deformation was in accordance with the direction of gravity (135° to 180° of the 2nd hinge, 0° to 45° of the 3rd hinge, 135° to 180° of the 4th hinge). The recovery time was going shorter and shorter from the 2nd hinge to the 4th hinge, specifically from 60 s to 56 s, the reason of which was that there was more weight to be supported during the recovery of the 2nd hinge, while only one short part of the tube did rotary movement during the 4th hinge recovery.

Satisfied shape memory performances of integrative hinge were observed through bending and shape memory recovery tests. Compared to about 60 s' recovery time of integrative SMPC hinge, traditional SMPC hinges need more time to deploy to the original state. Lan et al. reported a prototype of a solar array actuated by SMPC hinge, and it took about 100 s to deploy from 140° to 0° [33]. And another traditional SMPC hinge reported for space deployable structures took about 107 s to deploy fully [44]. In addition, the folding angle of traditional SMPC hinge is roughly from 120° to 140° depending on the cycle time and temperature, while folding angle of integrative SMPC hinge could reach 180° [44]. The integrative SMPC hinges are structural and functional integration without assembling process, and could avoid impact load to the system with simple and steady deploying process by comparison with mechanical deployable structures. Because mechanical deployable structures with spring hinge usually have complex and heavy connection parts [45–47], and may cause uncontrollable impact during the unfolding process, which could bring bad effects on surrounding components and parts.

5.5. Application

The prototype of deplorable structure has various applications in aerospace, such as self-driven gripping device, multi-angle imaging system and deployable solar array, and so on. Figs. 26 and 27 show a prospective self-driven gripping device and multi-angle imaging system that could be utilized in aerospace. The folded configuration of deplorable structure possesses superior mechanical properties and occupies little space, which enable to go through the launch stage of satellite. The deployed configuration makes it possible for the satellite to capture targets or record images of itself and space environment at working stage.

6. Conclusion

A SMPC based hinge, which is structural and functional integration without complex mechanical connections, has been designed and analyzed from the perspective of material, properties and application. The variable elastic modulus of SMPC with temperature has been obtained from tensile tests, providing evidence for simulation of bending property and modal analysis. Results from modal tests demonstrate the significantly improved structural total stiffness of integrative SMPC hinges, due to the higher natural frequencies. Bending behaviors such as strain and stress distributions, received from simulation data and DIC technique, are to evaluate the deformation process of integrated SMPC hinges. The hinges have satisfied shape memory recovery properties, including 100% shape recovery ratio with 10 times fold-deploy process and approximately 60 s shape recovery time from 180° to 0°. The integrated SMPC hinges can be applied to construct deployable structures for promising applications in aerospace, and two types of structures that are self-driven gripping device and multi-angle imaging system have been described. Further works will focus on the optimization design of structure, more precise experiments on whole structures and integration of multi-functional components for a wide range of application.

Acknowledgements

This work is supported by the National Natural Science Foundation of China (Grant No. 11632005, 11672086).

References

[1] Robinson P, Bismarck A, Zhang B, Maples HA. Deployable, shape memory carbon

fibre composites without shape memory constituents. Compos Sci Technol 2017;145.
[2] Liu T, Zhou T, Yao Y, Zhang F, Liu L, Liu Y, et al. Stimulus methods of multi-functional shape memory polymer nanocomposites: a review. Compos A: Appl Sci Manuf 2017;100.
[3] Meng Q, Hu J. A review of shape memory polymer composites and blends. Compos A Appl Sci Manuf 2009;40:1661–72.
[4] Glock S, Canal LP, Grize CM, Michaud V. Magneto-mechanical actuation of ferro-magnetic shape memory alloy/epoxy composites. Compos Sci Technol 2015;114:110–8.
[5] Wang W, Liu D, Liu Y, Leng J, Bhattacharyya D. Electrical actuation properties of reduced graphene oxide paper/epoxy-based shape memory composites. Compos Sci Technol 2015;106:20–4.
[6] Liu Y, Lv H, Lan X, Leng J, Du S. Review of electro-active shape-memory polymer composite. Compos Sci Technol 2009;69:2064–8.
[7] Lu H, Lei M, Zhao C, Yao Y, Gou J, Hui D, et al. Controlling Au electrode patterns for simultaneously monitoring electrical actuation and shape recovery in shape memory polymer. Compos B Eng 2015;80:37–42.
[8] Wei H, Liu L, Zhang Z, Du H, Liu Y, Leng J. Design and analysis of smart release devices based on shape memory polymer composites. Compos Struct 2015;133:642–51.
[9] Fabrizio Q, Loredana S, Anna SE. Shape memory epoxy foams for space applications. Mater Lett 2012;69:20–3.
[10] Hui L, Jing Z, Jing M, Xian G. The reinforcement efficiency of carbon nanotubes/shape memory polymer nanocomposites. Compos B Eng 2013;44:508–16.
[11] Lendlein A, Langer R. Biodegradable, elastic shape-memory polymers for potential biomedical applications. Science 2002;296:1673.
[12] Xiao X, Kong D, Qiu X, Zhang W, Liu Y, Zhang S, et al. Shape memory polymers with high and low temperature resistant properties. Sci Rep 2015;5:14137.
[13] Xie T. Recent advances in polymer shape memory. Polymer 2011;52:4985–5000.
[14] Yao Y, Wei H, Wang J, Lu H, Leng J, Hui D. Fabrication of hybrid membrane of electrospun polycaprolactone and polyethylene oxide with shape memory property. Compos B 2015;83:264–9.
[15] Wang X, Jiang M, Zhou Z, Gou J, Hui D. 3D printing of polymer matrix composites: a review and prospective. Compos B Eng 2017;110:442–58.
[16] Zhang R, Guo X, Liu Y, Leng J. Theoretical analysis and experiments of a space deployable truss structure. Compos Struct 2014;112:226–30.
[17] Zhao Q, Qi HJ, Xie T. Recent progress in shape memory polymer: new behavior, enabling materials, and mechanistic understanding. Prog Polym Sci 2015;49–50:79–120.
[18] Wei ZG, Sandstroröm R, Miyazaki S. Shape-memory materials and hybrid composites for smart systems: Part I Shape-memory materials. J Mater Sci 1998;33:3743–62.
[19] Blanco N, Gamstedt EK, Costa J. Mechanical hinge system for delamination tests in beam-type composite specimens. Compos Sci Technol 2008;68:1837–42.
[20] Sharafi S, Li G. Multiscale modeling of vibration damping response of shape memory polymer fibers. Compos B Eng 2016;91:306–14.
[21] Huang J, Zhang Q, Scarpa F, Liu Y, Leng J. Shape memory polymer-based hybrid honeycomb structures with zero Poisson's ratio and variable stiffness. Compos Struct 2017;179.
[22] Guo J, Wang Z, Tong L, Lv H, Liang W. Shape memory and thermo-mechanical properties of shape memory polymer/carbon fiber composites. Compos A Appl Sci Manuf 2015;76:162–71.
[23] Dastgerdi JN, Marquis G, Salimi M. The effect of nanotubes waviness on mechanical properties of CNT/SMP composites. Compos Sci Technol 2013;86:164–9.
[24] Leng J, Xie F, Wu X, Liu Y. Effect of the -radiation on the properties of epoxy-based shape memory polymers. J Intell Mater Syst Struct 2014;25:1256–63.
[25] Leng J, Lan X, Liu Y, Du S. Shape-memory polymers and their composites: stimulus methods and applications. Prog Mater Sci 2011;56:1077–135.
[26] Naito Y, Nishikawa M, Hojo M. Effect of reinforcing layer on shape fixity and time-dependent deployment in shape-memory polymer textile composites. Compos A 2015;76:316–25.
[27] Ohki T, Ni QQ, Ohsako N, Iwamoto M. Mechanical and shape memory behavior of composites with shape memory polymer. Compos A 2004;35:1065–73.
[28] Santo L, Quadrini F, Squeo EA, Dolce F, Mascetti G, Bertolotto D, et al. Behavior of shape memory epoxy foams in microgravity: experimental results of STS-134 mission. Microgravity Sci Technol 2012;24:287–96.
[29] Santo L, Quadrini F, Ganga PL, Zolesi V. Mission BION-M1: Results of RIBES/FOAM2 experiment on shape memory polymer foams and composites. Aerosp Sci Technol 2015;40:109–14.
[30] AIAA. Qualification of elastic memory composite hinges for spaceflight applications; 2006.
[31] Lake M, Munshi N, Meink T, Tupper M. Application of elastic memory composite materials to deployable space structures. AIAA Space 2001 Conference and Exposition; 2013.
[32] Yee JCH, Soykasap O, Pellegrino S. Carbon fibre reinforced plastic tape springs. Aiaa/asme/asce/ahs/asc Structures, Structural Dynamics & Materials Conference; 2004. p. 2000–54.
[33] Lan X, Liu Y, Lv H, Wang X, Leng J, Du S. Fiber reinforced shape-memory polymer composite and its application in a deployable hinge. Smart Mater Struct 2009;18:024002.
[34] Soykasap Ö. Folding design of composite structures. Compos Struct 2007;79:280–7.
[35] Wang W, Rodrigue H, Ahn SH. Deployable soft composite structures. Sci Reports 2016;6:20869.
[36] Akkus N, Kawahara M. Bending behaviors of thin composite pipes with reinforcing nodes. J Soc Mater Sci Jpn 2000;49:131–5.
[37] Leng J, Wu X, Liu Y. Effect of a linear monomer on the thermomechanical properties of epoxy shape-memory polymer. Smart Mater Struct 2009;18:7566–79.
[38] Zhang CS, Ni QQ. Bending behavior of shape memory polymer based laminates. Compos Struct 2007;78:153–61.
[39] Xia M, Takayanagi H, Kemmochi K. Analysis of multi-layered filament-wound composite pipes under internal pressure. Compos Struct 2001;53:483–91.
[40] Zhao W, Liu L, Lan X, Su B, Leng J, Liu Y. Adaptive repair device concept with shape memory polymer. Smart Mater Struct 2017;26:025027.
[41] Chen J, Liu L, Liu Y, Leng J. Thermoviscoelastic shape memory behavior for epoxy-shape memory polymer. Smart Mater Struct 2014;23:055025.
[42] Yang JS, Ma L, Schmidt R, Qi G, Schröder KU, Xiong J, et al. Hybrid lightweight composite pyramidal truss sandwich panels with high damping and stiffness efficiency. Compos Struct 2016;148:85–96.
[43] Yang JS, Xiong J, Ma L, Feng LN, Wang SY, Wu LZ. Modal response of all-composite corrugated sandwich cylindrical shells. Compos Sci Technol 2015;115:9–20.
[44] Dao TD, Ha NS, Goo NS, Yu WR. Design, fabrication, and bending test of shape memory polymer composite hinges for space deployable structures. J Intell Mater Syst Struct 2017. 1045389X774272.
[45] Jeong JW, Yoo YI, Lee JJ, et al. Development of a tape spring hinge with a SMA latch for a satellite solar array deployment using the independence axiom. Ieri Procedia 2012;1:225–31.
[46] Kim KW, Park Y. Systematic design of tape spring hinges for solar array by optimization method considering deployment performances. Aerosp Sci Technol 2015;46:124–36.
[47] Chen Z, Jiang X, Zhang X. Damped circular hinge with integrated comb-like substructures. Precis Eng 2018.